Fuel 304 (2021) 121378

Contents lists available at ScienceDirect

Fuel

journal homepage: www.elsevier.com/locate/fuel

Sustainable alternative fuel effects on energy consumption of jet engines

Randall C. Boehm *, Logan C. Scholla, Joshua S. Heyne

Department of Mechanical and Aerospace Engineering, University of Dayton, Dayton, OH 45469, USA

ARTICLE INFO

Keywords:
Jet fuel
Fuel composition
Waste heat recovery
Energy efficiency
Sustainable aviation fuel

ABSTRACT

High thermal stability enables engine manufacturers to increase the reliance on fuel as a heat sink while reducing the reliance on air, which wastes the energy used to compress it or increases aircraft drag. While the direct impact of waste heat recovery can translate into an energy savings of 0.2% if the maximum fuel temperature limit is increased to 160 °C (from 127 °C), there is a larger impact from a variety of options to improve the thermal efficiency of the engine. In this work, it is predicted that a combined savings of 0.5% or more is possible, 60% of which stems from leveraging the high thermal stability that synthetic fuels can afford. The engine performance and fuel system models that were developed to make these predictions, together with previously developed models to predict fuel properties from composition, have also been used in a series of Monte Carlo simulations to gage the impact of fuel composition variation on engine efficiency. A range of increased efficiency of 0.17% or 0.25% is predicted at high and low power, respectively. This works establishes a methodology to incorporate jet engine efficiency as an objective function in an algorithm designed to optimize sustainable alternative (jet) fuel composition.

1. Introduction

It has long been understood that increasing the reliance on jet fuel as a primary coolant for both the engine and the aircraft has significant performance and efficiency benefits relative to the use of air as a coolant [1], but fuel degradation and coking at high temperatures restricts how much heat can be put into the fuel. In some military applications, the performance benefits are significant enough to justify creating specialty fuels such as JP-7 and JPTS, which can tolerate much higher temperatures relative to petroleum-derived Jet A or Jet A-1 (JP-8) [2]. In land-based applications of gas turbines, weight is of little consequence so the operations of waste heat recovery (WHR) for plant efficiency or the cooling of combustor inlet temperature for emissions reduction can be accomplished in a wide variety of ways; all of which are impractical for flight because of the increased mass. Nonetheless, these applications provide some common examples of how controlling the air temperature along its flow path through the engine can have a large impact on performance, durability and energy efficiency [3]. Scientific research relating to fuel deoxygenation [4], and other ways to decrease the fuel coking or its impacts [5,6] may enable higher fuel heat sink capability with affiliated performance or efficiency benefits.

More recently, sustainable aviation fuels (SAF) have received attention because they are, or can be, part of high-priority geopolitical goals to (1) diversify energy supply chains and (2) reduce greenhouse gas emissions. Most of this attention has been around streamlining the evaluation processes to use synthetic fuels at some blend ratio with petroleum-derived jet fuel to create a so-called drop-in fuel that can be used within existing infrastructure without objection from any of the stakeholders [7]. However, there have also been discussions around characteristics of the SAFs and synthetic blend components (such as low aromatics, high specific energy [LHV], and high thermal stability) that make them attractive to consider as potential specialty fuels (such as JPTS) or high-performance fuels. As one example of high-performance fuels, Kosir et al. [8] recently published work highlighting the

Abbreviations: Sub 1, Engine intake, same pressure and temperature as ambient in this work; Sub 3, Compressor exit; Sub 36, Combustor intake; Sub 4, Combustor exit; ACOC, Air cooled, oil cooler; CDF, Cumulative distribution function; CDN, Combustor, diffuser, (stage 1, turbine) nozzle assembly; EPM, Engine performance model; FCAC, Fuel cooled, air cooler; FCOC, Fuel cooled, oil cooler; FS-SAF, Fully synthetic, sustainable aviation fuel; FSTM, Fuel system thermal model; H, Enthalpy; H/C, Hydrogen to carbon ratio (mole); LHV, Specific energy (lower heating value); P, Pressure or Power; SAF, Sustainable aviation fuel; T, Air temperature; TF, Fuel temperature; W, Air flow rate (mass); WF, Fuel flow rate (mass); WHR, Waste heat recovery; C_p, Heat capacity at constant pressure, per moles or mass; C_v, Heat capacity at constant volume, per moles or mass; P_{net}, Work extracted by turbine minus work put into compression, per unit time; γ, Ratio of heat capacities; ν, kinematic viscosity.

* Corresponding author.
E-mail address: rboehm1@udayton.edu (R.C. Boehm).

https://doi.org/10.1016/j.fuel.2021.121378
Received 17 March 2021; Received in revised form 1 July 2021; Accepted 2 July 2021
Available online 8 July 2021

efficiency gain expected from the use of fuels with high LHV, which all traces back to lower aircraft weight at take-off.

While the weight of the fuel onboard an aircraft is undoubtedly an essential component to the integrated engine-aircraft energy demand and efficiency, there is also expected to be an impact on the energy efficiency of the engine related to other properties of the liquid fuel, including:

1. H/C ratio: which, through its impact on combustor exhaust gas composition, has a small impact on the ratio of heat capacities (γ) and combustor exit temperature even when the total enthalpy created at the combustor is unchanged.
2. Viscosity impacts the heat transfer coefficients that ultimately determine how much waste heat is recovered by the fuel (coolant) and delivered back into the engine via the combustor.
3. Energy density impacts volumetric flow rates, which also impact heat transfer coefficients.
4. Specific heat also has some effect on heat transfer coefficients. Perhaps, more importantly, it also has a direct impact on the temperature rise in the fuel per unit of heat energy absorbed, which may impact the coking rate.
5. The coking rate (i.e., fuel thermal stability) drives several high-level design decisions relating to the thermal management of an engine.

To date, the synthetic blend component of approved alternative blend components are required to pass the ASTM D3241 thermal stability test at a test temperature of 325 °C (or higher, ASTM D7566) as compared to 260 °C for Jet A/A-1 (ASTM D1655). Therefore, it is expected that a fuel comprised exclusively of the synthetic blend component would exhibit substantially superior thermal stability relative to petroleum-derived fuels throughout the full range of conditions that the fuel would encounter in flight. Certain molecules, such as olefins, cyclopropanes, and cyclobutanes, have been excluded from consideration as components within a fully synthetic, drop-in, sustainable aviation fuel (FS-SAF) candidate because of concerns about their thermal oxidative stability.

In addition to those already mentioned, fuel composition influences all fuel properties, combustion figures of merit, and compatibility with materials and equipment used throughout the fuel handling and delivery systems, as has been discussed by Colket et al. [9]. Ultimately consideration must be given to all these dependencies prior to recommending a potential fuel for detailed evaluation as an aviation fuel, which is managed in this work by predicting all properties based on composition and filtering to the requirements of the fuel specifications.

There are three primary objectives of this work. Objective 1 is to assess the potential impact of FS-SAF to fuel energy consumption in a jet engine with no associated change in engine design or logic. Objective 2 is to assess the impact of leveraging the high thermal stability of FS-SAF candidates by increasing WHR up to a limit driven by the requirement that fuel vapor pressure must remain below the normal working fuel pressure at all operating conditions. Objective 3 is to assess the impact of fuel-cooled, cooling air [10] or reducing cooling air flow, as enabled by increasing the cooling load provided by the fuel.

2. Approach

At some high level, it can be argued that the maximum additional WHR is determined by the proposed shift in the maximum fuel temperature requirement: (160–127)*Cp where 160 °C is what we are proposing for high thermal stability fuels, 127 C is the requirement corresponding to petroleum-derived Jet A, and Cp is the heat capacity of the proposed fuel. While this is true at some level, it provides only part of the story. For this study, a fuel system thermal model (FSTM) was created as a tool to simulate the heat pick-up of fuel in real engines. This tool makes it possible to quantify the influence of fuel property variation on temperature rise and WHR within existing architectures. It also enables evaluations of conceptual level design changes that are intended to drive more heat into the fuel. A high-level engine performance model (EPM) was also created as a tool to evaluate and compare different conceptual designs that drive the same amount of total heat into the fuel (approximately 33*Cp more than baseline) but taking that heat from different sources. The EPM also enables the evaluation of H/C impact on combustor exit temperature and turbine work extraction, which is usually neglected in performance models because it is perceived to be insignificant and the H/C of fuel onboard an aircraft is not generally known. Weight, including fuel and hardware differences, is also an important factor in overall system efficiency. It is evaluated here strictly to facilitate contextual comparison for the engine-level efficiencies we report. For this estimate, the fuel weight is 30% of the baseline, total system weight of 40,000 kg; applied to both operating conditions that are considered.

A distribution of properties for FS-SAF candidates is created by virtually blending individual molecules by random association of mole fractions, whose values are also randomly determined, to each of eighty-nine specific molecules with known physical and chemical properties [11]. Each chemical and physical property of a mixture is derived from the mixture definition and constituent properties according to ideal mixture blending rules and are documented elsewhere [8]. A trial guess at a FS-SAF candidate is then passed through a filter to determine whether it is expected to pass ASTM D1655 and ASTM D7566 fuel specifications. If it passes this filter, it is included within the distribution that is input to the FSTM and EPM as part of a Monte Carlo simulation. The total enthalpy supplied to the engine per unit time is conserved in these simulations, except where fuel savings are determined. To calculate fuel savings, the fuel flow of the more efficient case is reduced until the net work per unit time (P_{net}) - expansion plus compression is conserved. Additional description of the virtual fuel creation and definition can be found in the works of Kosir et al. [12,13]. All liquid fuel properties include first-order temperature dependence, and none include pressure dependence.

The FSTM is comprised of 5–6 elements as shown in Fig. 1. The hydraulic diameter of the tubing and heat exchanger passages was set equal to 1.9 and 1.5 cm, respectively, while the length of each element was adjusted to yield a temperature rise corresponding to experienced-based expectations. The hot side temperature was held constant in each heating element. The inlet fuel temperature to element 1 corresponds to a heat-soaked engine in a hot and harsh environment. The outlet temperature of the fuel pump, element 2, was adjusted through manual iteration until a small positive temperature rise was achieved. All of the remaining values were determined by one-dimensional heat transfer analyses using the correlations of Talar [14] for straight tubes (elements 1, 3 & 4) or Gneilinski [15] for coils (elements 5 & 6). Temperature-dependent fluid properties were based on the average temperature (T_{bulk}) of each element and the calculated wetted wall temperature (T_{ww}). The radial heat flux into the fluid, which scales with ($T_{ww} - T_{bulk}$) and the radial heat flux through the metal, which scales with ($T_{hot} - T_{ww}$) were made equal, and these were made equal to the axial heat flux per unit length across the element, which scales with ($T_{outlet} - T_{inlet}$). This model, along with the boundary conditions shown in Table 1, were used to determine the WHR by the fuel coolant for the purpose of assessing the impact of fuel property variations.

The EPM is comprised of a 2-stage compressor, a combustor, and a turbine, as shown in Fig. 2. For simplicity, all air flow that is taken off the compressor and used for cooling is assumed to do no work as it expands. Output from the FSTM enters the EPM through the combustor and includes WF_{36}, WHR, and the temperature of the reference fuel at inlet to the combustor. The heat available (H_{avail}) to raise the temperature of the combustion products from the temperature at the exit of the compressor (T_3) to the temperature at the entrance to the turbine (T_4) is given by Equation (1). A configuration is defined by the set of assumptions, boundary conditions, and options that complete the EPM. Table 2 provides a compilation of the boundary conditions applied to the EPM for

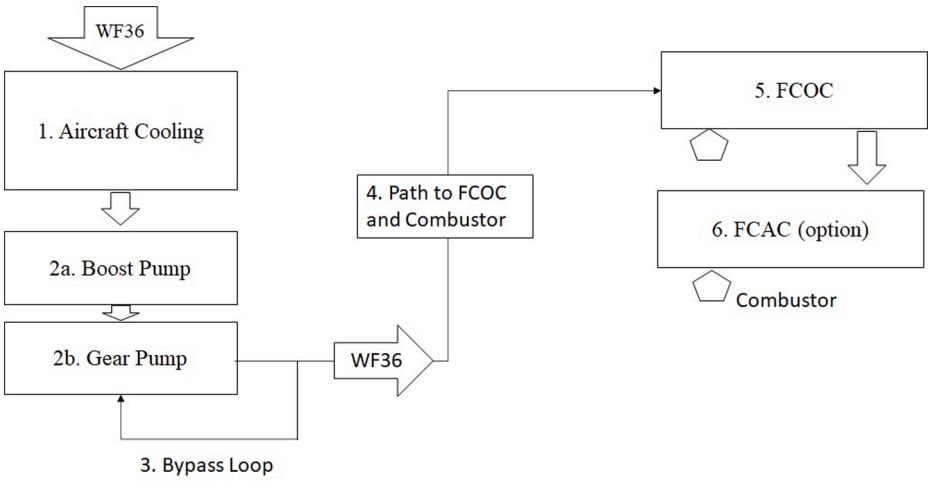

Fig. 1. FSTM Block Diagram. The optional 6th element is a fuel-cooled air cooler.

Table 1
FSTM Boundary Conditions. Fuel flow rate varies from fuel to fuel to hold enthalpy flux (WF_{36}*LHV) constant. The values shown correspond to the reference fuel, A2.

Element	Low Power			High Power		
	Inlet T,° C	Hot Side T, °C	WF, kg/s	Inlet T, °C	Hot Side T, °C	WF, kg/s
1	36.85C	56.85	0.05	36.85	61.85	1.00
2	calculate	n/a	0.50	calculate	n/a	1.025
3	64.85	66.85	0.45	43.85	76.85	0.025
4	64.85	116.85	0.05	43.85	126.85	1.00
5	calculate	169.85	0.05	calculate	169.85	1.00
6	calculate	184.61 (T_3)	0.05	calculate	527.34 (T_3)	1.00

this investigation.

$$H_{avail} = W_f{*}LHV + H_{fuel,T_f} + H_{air,T_3} - H_{products,T_3} \quad (1)$$

$$where H_{air,T_3} = W_{36}{*}\int_{25}^{T3} C_{p,air}$$

$$H_{products,T_3} = (W_{36} + W_f){*}\int_{25}^{T3} C_{p,products}$$

$$and H_{fuel,T_f} = W_f{*}\int_{25}^{T_f} C_{p,fuel} = \Delta WHR + W_f{*}\int_{25}^{T_{f,baseline}} C_{p,ref\_fuel}$$

The Monte Carlo simulations of 2500 potential fuels were carried out at two different mission conditions and two different engine model configurations. The low power mission condition is intended to approximate the chop from cruise to flight idle, where air and fuel flow are low because of the high altitude and low thrust demand. The engine temperatures are in transition between steady-state cruise and pseudo-steady-state flight idle. The peak fuel temperature in jet engines is observed during this transition on a hot day. The high power mission condition is intended to represent the opposite extreme of the operating envelope and is marked by 10 times more air flow and 20 times more

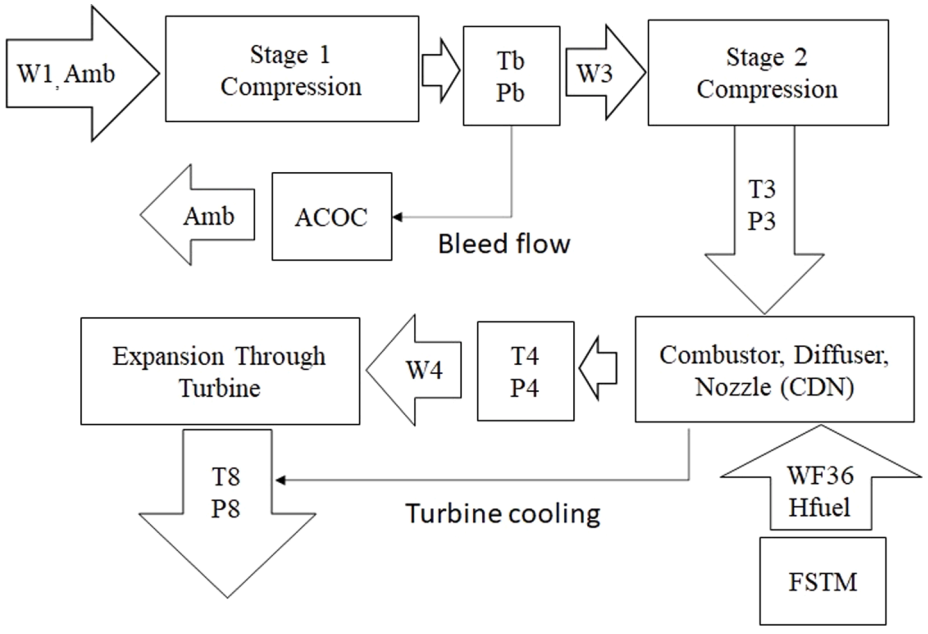

Fig. 2. EPM Block Diagram.

Table 2
EPM Boundary Conditions.

Pressure Ratios (relative to ambient)	Low Power	High Power
Stage 1 Compression	1.02	6.25
Stage 2 Compression	6.53	40.00
Turbine	1.10	2.00
Ambient Conditions		
Pressure, kPa	49.1	101
Temperature, °C	−4.65	15
Altitude, m	6100	0
Air Flows (kg/s)		
W_3	4.9	49.43
ACOC bleed	0.10	0.57
Turbine cooling	30% of W_3	30% of W_3
Other Inputs		
CDN loss (P_4/P_3)	0.94	0.94
Compressor efficiency	1.00	1.00
Turbine efficiency	0.70	0.70
Options	No ACOC Larger FCOC	FCAC Reduced turbine cooling

fuel flow relative to the low power condition. The baseline EPM does not include any of the design options listed at the bottom of Table 2 and is intended to represent generally, an in-service jet engine. The derivative engine model configuration includes a fuel-cooled air cooler that is sized to raise the temperature of our reference jet fuel (called A2, consistent with several other research groups [9,16]) by 33 °C. The turbine cooling flow split is reduced enough to conserve the amount of heat it absorbs from the hot turbine components at high power. Three additional engine model configurations were evaluated at both high and low power using the reference fuel, and these results will be discussed at the end of the next section.

3. Results

This section first compares selected results of the baseline engine model configuration and the derivative engine model configuration. These results are followed by a discussion of fuel impact on energy consumption summarized by cumulative distribution functions shown for each of the four cases. Included within this discussion is a sensitivity analysis to highlight which fuel properties have the most significant impact on energy efficiency at the engine level. These properties are contrasted against other figures of merit, such as thermal stability, particulate emissions, and fuel weight/aircraft efficiency. Finally, a comparison is made between various ways to reduce air cooling flows or optimize the benefit of cooled cooling air.

In Table 3, a summary is provided of the FSTM results using fuel properties corresponding to the reference fuel, A2. The data in the rows corresponding to elements 1–5 are the same for both engine model configurations, while the data in the row corresponding to element 6 represents the derivative engine model configuration which includes a fuel-cooled air cooler. At low power, the flow in element 1 is laminar for most fuels and turbulent in element 5 despite a common flow rate because Reynolds number (Re) varies inversely with viscosity, which decreases exponentially as fuel temperature increases from station to station, along the flow path. The overall fuel temperature rise for the baseline configuration at low power (86.3 °C) is consistent with real engine experience. The flow velocity is high at high power, rendering it fully turbulent in elements 1, 4, 5, and 6 for all fuels. While the heat extracted from the surrounding metal at high power is 6 times more than is extracted at low power, the flow rate is 20 times higher. Therefore, the change in fuel temperature at high power is much less than it is at low power. With the reduced range of fuel temperature and fully turbulent flow, it should be expected that high power will reveal different fuel dependencies than low power. The bypass loop, element 3, has high flow at low power and low flow at high power to accommodate a gear pump for which the flow rate difference between low and high power is much lower than the difference in flow rate to the engine. The low flow rate in this element at high power does, in fact, lead to a significant increase in fuel temperature, but once mixed with the main engine flow, its impact is washed out. The reverse is true at low power. This is why the results show the pump inlet temperature to be nearly equal to the element 1 (aircraft fuel system) exit temperature at high power and nearly equal to the bypass loop exit temperature at low power.

Table 3
FSTM results summary. Underlined text represents model input. See Fig. 1 for a definition of the element numbers.

Element	Low Power			High Power		
	Inlet T, °C	Exit T, °C	WHR, kW	Inlet T, °C	Exit T, °C	WHR, kW
1	36.85	49.95	1.36	36.85	42.64	11.9
2	64.25	64.85	0.65	42.77	43.85	2.30
3	64.85	65.79	0.92	43.85	90.92	0.26
4	64.85	111.68	5.33	43.85	62.95	40.6
5	111.68	123.16	1.37	62.95	65.28	5.05
Baseline total	36.85	123.16	9.65	36.85	65.28	60.0
6	123.16	160.04	4.62	65.28	100.59	79.5
Derivative total	36.85	160.04	14.27	36.85	100.59	139.4

The fuel-cooled air cooler is sized such that the fuel temperature will not exceed 160 °C at the low power condition. The air temperature at the exit of the compressor (T_3) is 184.6 °C at this condition, which is lower than a real engine would have for the same pressure ratio because we have assigned an efficiency of 1.0 to the compressor in the EPM. The temperature of the reference fuel at the exit of element 5 (TF_{FCOC}) at this condition is 123.2 °C, and the target fuel temperature at the entrance to the combustor (TF_{36}) is 160 °C. To gauge whether this target temperature is realistic, given the model assumptions, the temperature at thermal equilibrium was calculated for comparison, see Equation (2). To achieve the goal of 160 °C fuel temperature, the fuel-cooled air cooler will have to achieve 65% transference of the available heat. Not surprisingly, the fuel-cooled air cooler created for this study is substantially larger (3.75 times) than the fuel-cooled oil cooler.

$$T_{EQ} = \frac{\left(W_{cool} * C_{p,air} * T_3 + WF_{36} * C_{p,A2} * TF_{FCOC}\right)}{\left(W_{cool} * C_{p,air} + WF_{36} * C_{p,A2}\right)} = 180.0^{\circ}\mathrm{C} \quad (2)$$

At high power, the heat transferred from the air to the fuel in the fuel-cooled air cooler is driven by a much more significant heat difference between the two fluid streams because T_3 is much higher (527.3 vs. 184.6 °C) and TF_{FCOC} is much lower (65.3 vs. 123.2 °C). This large forcing factor at high power, together with the large heat exchanger leads to ~3 times more heat transferred in this one heat exchanger than the entirety of the legacy fuel system, which is driven by a hot-side metal temperature no greater than 170 °C. In the baseline engine model configuration, the WHR is small relative to the fuel LHV: 0.14% at high power and 0.45% at low power. In the derivative engine model configuration, the ratio of WHR to LHV is 0.32% and 0.66% at high and low power, respectively. It is anticipated, therefore, that fuel properties that influence WHR will have more impact on energy consumption for the derivative engine than the baseline engine and more impact at low power than at high power. Regardless of the conversion of WHR into useful work by the turbine, it is already obvious that leveraging the fuel thermal stability is important.

Fuel effects on combustor performance are manifested through differences in WHR and exhaust gas C_p. WHR is a direct adder to the enthalpy stored in the exhaust gas, while C_p influences T_4 for a given enthalpy. Higher C_p leads to lower T_4, which may have some small impact on hot section life, not considered here, but does not otherwise influence the combustor performance. Efficiency losses in the CDN arise from two primary sources, pressure losses (6%) and bleed flow to cool the turbine. The loss arising from the bleed flow is calculated by

multiplying the total work done by the compressor on the air that enters the combustor by the cooling air flow split (1-W_{36}/W_3). The loss arising from CDN pressure drop is calculated by running the turbine module at the higher and lower exit pressure. Fuel properties have no impact on the loss associated with cooling flow, and little impact (via the influence on turbine performance) on the loss associated with CDN pressure drop.

The performance (*Pow*) of the turbine depends on combustor exhaust gas temperature (T_4), pressure (P_4), density (or molecular weight), and heat capacity at constant pressure (C_p) and volume (C_v), as described by Equation (3).

$$Pow = W_4 * \int_{T4}^{T8} dH = W_4 * \int_{T4}^{T8} C_p dT \approx W_4 * \overline{C_p} * (T_8 - T_4)$$
$$= W_4 * \overline{C_p} * T_4 * \left[\left(\frac{P8}{P4} \right)^{\frac{\gamma-1}{\gamma}} - 1 \right] \quad (3)$$

where $\gamma = \frac{Cp}{Cv}$ of the burnt gas, and is determined at $(T_8 + T_4)/2$.

While the composition of the exhaust gas is ~80% nitrogen for all cases, differences in fuel to air ratio and fuel H/C do have an impact, as shown in Table 4, where low H/C is favorable to turbine performance. The H/C values shown in this table correspond to the opposite ends of the range represented in our simulations using the baseline engine model configuration. The composition effect is more evident at high power than low power because the turbine inlet temperature is higher. More importantly, the fuel to air ratio (F/A) is twice as high. The same combination of fuel properties also influences the performance of exhaust nozzles, not included here, and those effects are expected to offset the fuel effects on turbine performance partially. More importantly, fuel weight scales inversely with H/C unless it contains a significant fraction of strained cycloparaffins or reactive species that may lead to poor thermal stability. For the range of H/C values covered in this work, the correlated fuel weight varies by 2.7%, which would lead to an efficiency reduction at the system level of 1.6%. Hence, the practical impact of H/C on turbine power extraction (see Table 4) is small relative to its impact on system-level efficiency, arising from its impact on fuel weight.

Low H/C fuel is also a risk to both soot formation during combustion and coking within the fuel system. The sooting risk is managed by predicting the threshold sooting index based on fuel composition and requiring it to pass a filter on this property that is analogous to the smoke point limit quoted in fuel specifications. The coking risk is partially managed by excluding all at-risk species from the database used to construct the trial fuels, but ultimately needs further assessment.

When the engine model is reconfigured to exploit the higher thermal stability of FS-SAF, the savings relative to the baseline engine model configuration is substantial. The derivative engine model configuration consumes 0.5% less energy than the baseline model at both high and low power. Forty percent of that savings originates from the recovered waste heat (79.5 kW, high power or 4.6 kW, low power) that is delivered to the combustor via elevated fuel enthalpy, and sixty percent originates from the reduction of turbine cooling flow from 30.00% of W_3 to 29.75%. It is important to recognize that FS-SAF with high thermal stability may not be the only way to enable a higher heat sink. Qualified fuel additives, such as the so-called '+100' additive cocktail, can reduce deposition of thermal oxidation products [5], removal of dissolved oxygen gas can reduce thermal oxidation [4], and coke barrier coatings [6] can embrittle coke deposits, causing them to spall prior to growing large enough to materially impact the operation of the engine. The derivative engine described here could burn FS-SAF or Jet-A + 100 interchangeably and would be tolerant of some infrequent exposure to petroleum-derived fuel without the thermal stability additive. The other two strategies seek to enable higher fuel heat sink capability by additional hardware changes and are not proven technologies despite nearly two decades of development opportunity.

To help identify which impacts are larger and where the savings are realized, a compilation of major heat elements is provided in Table 5. Expansion through the turbine is the largest heat element and the only one (of those listed) that is significantly impacted by fuel properties directly. Obviously, the enthalpy supplied to the turbine is directly proportional to the fuel enthalpy supplied to the combustor, as discussed earlier. Fig. 3 presents a graphical perspective on fuel energy savings as a function of fuel composition, engine operating condition, and engine model configuration. The fuel composition impact is largest (0.25%) at low power for the baseline configuration, where the skewed population distribution reveals the deleterious effect of high viscosity and non-turbulent flow at the low-efficiency end. At high power, the H/C ratio (i.e., exhaust gas composition) is primarily responsible for the observed variation in energy savings (0.17%), while WHR and H/C are both significant at low power. Relative to the heat supplied to the combustor at high power, the variation in WHR caused by fuel composition variation is small, as is readily apparent by the nearly vertical cumulative population distributions (CDF's) shown in Fig. 4, and this explains why WHR does not contribute to the width of the CDF's corresponding to high power when plotted against energy savings (Fig. 3). The shapes of the CDF's shown in Fig. 4 are not changed between the baseline and derivative engine model configurations, and a deeper look into the data beneath these distributions shows a similar ranking of simulated fuels. This is important because it suggests that a fuel that is ideal for one engine will also be good for any engine, if not optimal. The ranking of simulated fuel does not, however, hold for the different operating conditions, which suggests that a representative mission mix should be used to assess the fuel impact on energy efficiency when formulating optimized fuel. The results of a linear regression statistical analysis, as summarized in Fig. 5, provides another way of summarizing these points.

Because WHR is significant, it is useful to understand which fuel properties have the largest impact on it. While it can be argued that the heat transfer correlations already describe these dependencies in detail, they do not account for the linkage between composition and the physical properties. In this work, we found that viscosity variation is the most important factor influencing waste heat recovery at low power, where its impact on energy efficiency is the largest. Heat capacity per unit volume and energy density contribute to a lesser degree. These results are summarized in Fig. 6. Ideally, to maximize WHR, a fuel would have low viscosity (high Re), low energy density (high flow velocity), and high heat capacity per unit volume. With optimal exhaust gas composition (represented by H/C) and fuel weight (represented by LHV), there are five properties to optimize simultaneously. The dimensionality of this optimization can be reduced to two by using the

Table 4
Impact assessment of H/C variation on turbine power extraction.

H/C	F/A	T_4, K	$C_p(T_4)$, kJ/kg	γ (T_4)	Power / W_4, MJ/kg
2.102	0.0289	1749.2	1.2425	1.3003	1.102
1.763	0.0289	1754.1	1.2354	1.3026	1.1041
2.102	0.0146	1014.9	1.1282	1.3412	0.4169
1.763	0.0146	1016.2	1.1254	1.3423	0.4173

Table 5
Summary of major heat terms for selected configurations. Fuel properties influence the expansion term.

Power	High		Low	
Hardware Configuration	Baseline	Derivative	Baseline	Derivative
ACOC bleed loss	0.11 Mw	0.11	0.15 kW	0.15
CDN pressure loss	0.55 Mw	0.55	40 kW	41
Turbine cooling loss	7.92 Mw	7.77	281 kW	276
Turbine-aero loss	11.79 Mw	11.82	435 kW	437
Compression	26.5 Mw	26.5	937 kW	937
Expansion	27.5 Mw	27.6	1016 kW	1019
P_{net}	0.97 Mw	1.05	78.8 kW	81.6
Savings	Reference	0.47%	Reference	0.52%

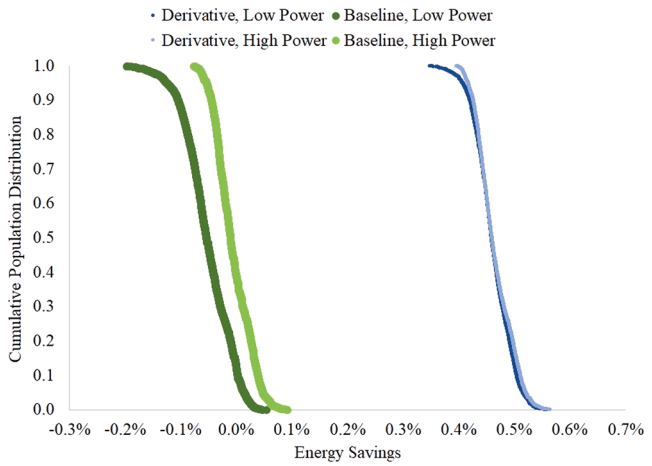

Fig. 3. Design and fuel property dependencies on fuel energy savings.

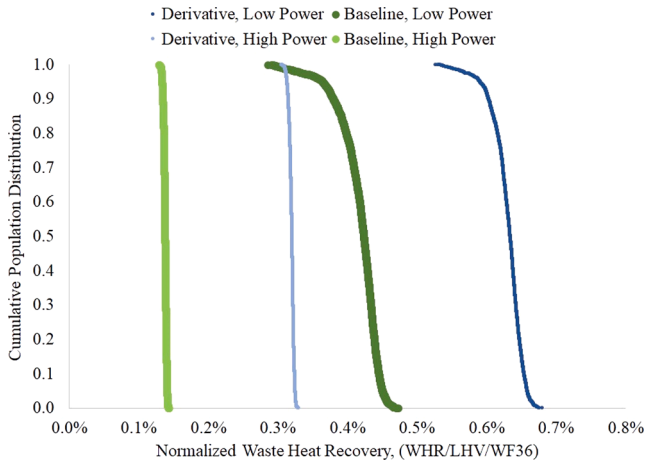

Fig. 4. Design and fuel property dependencies on waste heat recovery.

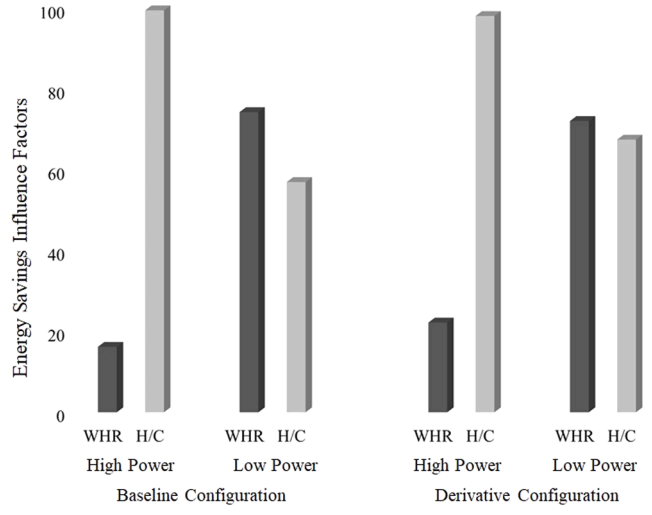

Fig. 5. Influence factors on energy savings variation caused by fuel composition variation. R^2 is 0.99 or higher for each case.

models described in this work to treat energy efficiency at the engine level as one property to optimize and system weight as the other. Potentially a single objective function (sometimes called, 'cost function'), representing aircraft energy efficiency could be derived, but the

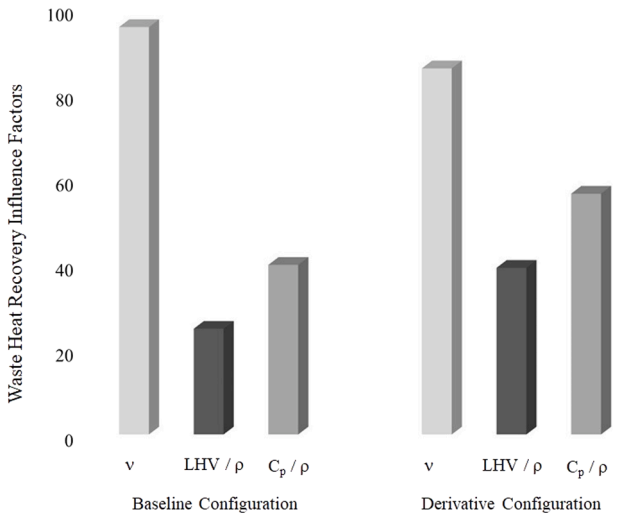

Fig. 6. Influence factors on waste heat recovery variation at low power, caused by fuel composition variation. R^2 of linear regression is 0.94–0.95.

fuel weight impact on drag depends on its fraction of the total aircraft weight, which depends on the aircraft, its mission, and how much excess fuel is onboard the aircraft. Because of these complications, we intend to retain two objective functions going forward in the near term.

Returning now to a quantification of the impact of improved thermal stability on engine energy consumption, the derivative engine model configuration (B) that has been discussed above is not the only option. Many options are possible, three of which have been considered in this work: C) increasing the size of the fuel-cooled, oil cooler and eliminating the air-cooled, oil cooler, D) adding a fuel-cooled, air cooler as was done for the derivative engine model configuration but keeping the same turbine cooling flow as the baseline engine model configuration, and E) similar to the one above, but use the cooled cooling air to improve the turbine efficiency by an arbitrary amount (0.1%). All options lead to an energy savings at the engine level that is significantly higher than the impact of fuel properties alone, a summary of which is provided in Fig. 7. It is important to note these numbers all depend on the maximum allowable fuel temperature on-wing. Greater energy savings is possible if the engine were to operate exclusively on FS-SAF with high thermal stability and high initial boiling point, subject to the temperature limitation of elastomeric seals or other components within the fuel system. While option C would result in a small weight decrease, the other

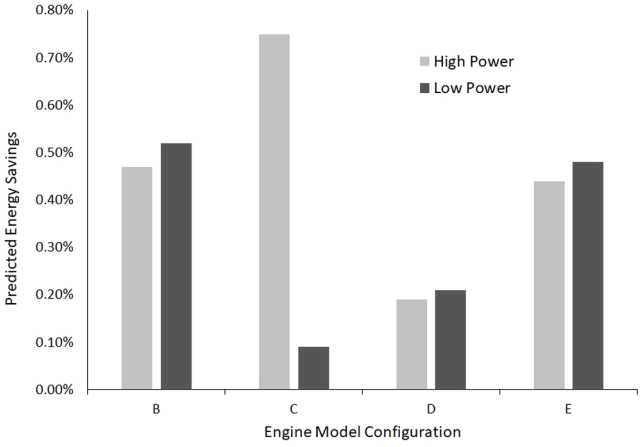

Fig. 7. Summary of predicted energy savings for a variety of engine model configurations. B. Cooled cooling air with reduced cooling flow. C. Enlarged fuel-cooled, oil cooler in place of air-cooled, oil cooler. D. Cooled cooling air alone. E. Cooled cooling air and improved turbine efficiency (0.700 to 0.701).

options considered all lead to a small weight increase. A rough order of magnitude estimate of this increase is 5 kg per engine, which would erode 0.05% from the stated benefits for options B, D & E, as shown in Fig. 7.

4. Conclusion

This work establishes a methodology to treat jet engine energy efficiency as an objective function in an algorithm designed to optimize sustainable aviation fuel composition. The methodology has been used here to satisfy three research objectives. Objective 1: Without any associated change to the engine model configuration, on-spec fuel composition variation can lead to ~0.2% variation in engine efficiency at both high and low power, mostly resulting from H/C variation at high power and a combination of H/C variation and viscosity variation at low power. Relative to nominal Jet-A fuel, the best fuel among 2500 random samples created from the pilot-scale database of 89 compounds shows a 0.05% benefit at low power and a 0.11% benefit at high power. Objective 2: The high thermal stability of fully synthetic fuel can be leveraged by making design changes within the thermal management systems on an engine to drive more heat into the fuel. Without sacrificing the capability to burn any on-spec Jet-A fuel infrequently, should the supply chain of the synthetic fuel be interrupted, the predicted energy savings that would result from this change is 0.2% at both high and low power. Objective 3: By increasing the reliance on fuel as a coolant onboard the aircraft, (parasitic) cooling air flow can be reduced or potentially eliminated altogether. While this benefit varies with design choices, it is reasonable to claim 0.3%.

Finally, two very important observations were made during this investigation. One: The first objective has low sensitivity to the choice of engine model configuration, hinting that a fuel that has been optimized for one configuration will likely be optimal for all configurations, but the magnitude of the impacts would likely be different. Two: The first objective is sensitive to the choice of operating condition, suggesting that is important to include a representative mix of operating conditions (a mission mix) as part of the objective function in subsequent optimizations of the fuel composition.

CRediT authorship contribution statement

Randall C. Boehm: Conceptualization, Methodology, Software, Formal analysis, Data curation, Writing - original draft, Writing - review & editing. **Logan C. Scholla:** Software, Data curation. **Joshua S. Heyne:** Project administration, Funding acquisition, Writing - review & editing.

Declaration of Competing Interest

The authors declare that they have no known competing financial interests or personal relationships that could have appeared to influence the work reported in this paper.

Acknowledgements

This research was funded by the U.S. Federal Aviation Administration Office of Environment and Energy through ASCENT, the FAA Center of Excellence for Alternative Jet Fuels and the Environment, project 66 through FAA Award Number 13-C-AJFE-UD-027 under the supervision of Dr. Anna Oldani. Any opinions, findings, conclusions or recommendations expressed in this material are those of the authors and do not necessarily reflect the views of the FAA.

References

[1] Bruening GB, Chang WS. Cooled cooling air systems for Turbine thermal management. Proc ASME Turbo Expo 1999;3. https://doi.org/10.1115/99-GT-014.
[2] Edwards T. Advancements in gas turbine fuels from 1943 to 2005. J Eng Gas Turbines Power 2007;129:13–20. https://doi.org/10.1115/1.2364007.
[3] Wilfert G, Sieber J, Rolt A, Baker N, Touyeras A, Colantuoni S. New Environmental Friendly Aero Engine Core Concepts. ISABE-2007-1120. 18th Int Symp Air Breath Engines 2007:1–11.
[4] Zabarnick S, West ZJ, Arts A, Griesenbrock M, Wrzesinski P. Studies of the impact of fuel deoxygenation on the formation of autoxidative deposits. Energy Fuels 2020;34(11):13814–21. https://doi.org/10.1021/acs.energyfuels.0c0260310.1021/acs.energyfuels.0c02603.s001.
[5] Heneghan SP, Zabarnick S, Ballal DR, Harrison WE. JP-8+100: The development of high-thermal-stability jet fuel. J Energy Resour Technol Trans ASME 1996;118:170–9. https://doi.org/10.1115/1.2793859.
[6] Mancini AA, Ackerman JF, Richard LK, Stowell WR. Method and Coating System for Reducing Carbonaceous Deposits on Surfaces Exposed to Hydrocarbon Fuels at Elevated Temperatures. 6808816 B2, 2004.
[7] Colket M, Heyne J, Rumizen M, Gupta M, Edwards T, Roquemore WM, et al. Overview of the National Jet Fuels Combustion Program. AIAA J 2017;55(4):1087–104. https://doi.org/10.2514/1.J055361.
[8] Kosir ST, Behnke L, Heyne JS, Stachler RD, Flora G, Zabarnick S, et al. Improvement in jet aircraft operation with the use of high-performance drop-in fuels. AIAA Scitech 2019. Forum 2019. https://doi.org/10.2514/6.2019-0993.
[9] Colket M, Heyne J. Fuel Effects on Operability of Aircraft Gas Turbine Combustors. submitted. AIAA,. Progress in Astronautics and Aeronautics; 2021.
[10] Deveau PJ, Greenberg PB, Paolillo RE. Gasturbine Engine Active Clearance Control. 4513567, 1985.
[11] Lemmon, E.W., Bell, I.H., Huber, M.L., McLinden MO. NIST Standard Reference Database 23: Reference Fluid Thermodynamic and Transport Properties-REFPROP 2018.
[12] Kosir S, Heyne J, Graham J. A machine learning framework for drop-in volume swell characteristics of sustainable aviation fuel. Fuel 2020;274:117832. https://doi.org/10.1016/j.fuel.2020.117832.
[13] Kosir S, Stachler R, Heyne J, Hauck F. High-performance jet fuel optimization and uncertainty analysis. Fuel 2020;281:118718. https://doi.org/10.1016/j.fuel.2020.118718.
[14] Taler D, Taler J. Determining heat transfer correlations for transition and turbulent flow in ducts. Sci Lett Rzesz Univ Technol – Mech 2014;31(86(1/2013)):103–14. https://doi.org/10.7862/rm10.7862/rm.2014.12.
[15] Gnielinski V. Heat transfer and pressure drop in helically coiled tubes. Proc. 8th Int. Heat Transf. Conf., San Francisco: Hemisphere; 1986, p. 696.
[16] Edwards T. Reference Jet Fuels for Combustion Testing. 55th AIAA Aerosp Sci Meet 2017:1–58. doi: 10.2514/6.2017-0146.

Technical Report Documentation Page

1. Report No.	2. Government Accession No.	3. Recipient's Catalog No.
j.fuel.2021.121378		

4. Title and Subtitle	5. Report Date
Sustainable alternative fuel effects on energy consumption of jet engines	July 2021
	6. Performing Organization Code

7. Author(s)	8. Performing Organization Report No.
Randall C. Boehm, Logan C. Scholla, Joshua S. Heyne	

9. Performing Organization Name and Address	10. Work Unit No. (TRAIS)
Center of Excellence for: Alternative Jet Fuels and Environment Department of Mechanical and Aerospace Engineering University of Dayton, Dayton, OH 45469, USA	11. Contract or Grant No. 13-C-AJFE-UD-027

12. Sponsoring Agency Name and Address	13. Type of Report and Period Covered
Federal Aviation Administration Office of Environment and Energy	Journal Article
	14. Sponsoring Agency Code

15. Supplementary Notes

16. Abstract

High thermal stability enables engine manufacturers to increase the reliance on fuel as a heat sink while reducing the reliance on air, which wastes the energy used to compress it or increases aircraft drag. While the direct impact of waste heat recovery can translate into an energy savings of 0.2% if the maximum fuel temperature limit is increased to 160 ◦ C (from 127 ◦ C), there is a larger impact from a variety of options to improve the thermal efficiency of the engine. In this work, it is predicted that a combined savings of 0.5% or more is possible, 60% of which stems from leveraging the high thermal stability that synthetic fuels can afford. The engine performance and fuel system models that were developed to make these predictions, together with previously developed models to predict fuel properties from composition, have also been used in a series of Monte Carlo simulations to gage the impact of fuel composition variation on engine efficiency. A range of increased efficiency of 0.17% or 0.25% is predicted at high and low power, respectively. This works establishes a methodology to incorporate jet engine efficiency as an objective function in an algorithm designed to optimize sustainable alternative (jet) fuel composition.

17. Key Words	18. Distribution Statement
Jet fuel, Fuel composition, Waste heat recovery, Energy efficiency, Sustainable aviation fuel, ASCENT	

19. Security Classif. (of this report)	20. Security Classif. (of this page)	21. No. of Pages	22. Price
Unclassified	Unclassified		